Front. Electr. Electron. Eng. China 2009, 4(1): 104–113
DOI 10.1007/s11460-009-0010-5

RESEARCH ARTICLE

Yinshun WANG, Xiang ZHAO, Junjie HAN, Huidong LI, Yin GUAN, Qing BAO, Xi XU, Shaotao DAI, Naihao SONG, Fengyuan ZHANG, Liangzhen LIN, Liye XIAO

Development and test in grid of 630 kVA three-phase high temperature superconducting transformer

Abstract A 630-kVA 10.5 kV/0.4 kV three-phase high temperature superconducting (HTS) power transformer was successfully developed and tested in a live grid. The windings were wound by hermetic stainless steel-reinforced multi-filamentary Bi2223/Ag tapes. The structures of primary windings are solenoid with insulation and cooling path among layers, and those of secondary windings consist of double-pancakes connected in parallel. Toroidal cryostat is made from electrical insulating glass fiber reinforced plastics (GFRP) materials with room temperature bore for commercial amorphous alloy core with five limbs. Windings are laid in the toroidal cryostat so that the amorphous core operates at room temperature. An insulation technology of double-half wrapping up the Bi2223/Ag tape with Kapton film is used by a winding machine developed by the authors. Fundamental characteristics of the transformer are obtained by standard short-circuit and no-load tests, and it is shown that the transformer meets operating requirements in a live grid.

Keywords high temperature superconducting (HTS) transformer, Bi2223/Ag tape, amorphous alloy, windings, liquid nitrogen

Translated from *Proceedings of the CSEE*, 2007, 27(27): 24 –31 [译自: 中国电机工程学报]

Yinshun WANG (✉), Huidong LI, Yin GUAN, Qing BAO, Xi XU, Shaotao DAI, Naihao SONG, Fengyuan ZHANG, Liangzhen LIN, Liye XIAO
Institute of Electrical Engineering, Chinese Academy of Sciences, Beijing 100080, China
E-mail: yswang@ncepu.edu.cn

Xiang ZHAO, Junjie HAN
Technical Center of Tebian Electric Apparatus Stock Co., Ltd, Changji 831100, China

Yinshun WANG
Beijing Key Laboratory of High Voltage and EMC, School of Electrical and Electronic Engineering, North China Electric Power University, Beijing 102206,China

1 Introduction

With the development of high temperature superconducting (HTS) tapes, HTS tape properties have been greatly improved in terms of critical current, mechanical and uniformity. In recent years, practical HTS tapes have been realized commercially and made great progress in electrical power application [1]. Applications such as HTS cables [2,3], transformers [4–6], fault current limiters (FCL) [7,8], generators and motors [9], and superconducting magnetic energy systems (SMESs) [10], etc. were successively tested in a live grid.

HTS transformers have advantages over conventional transformers that include low loss, improved efficiency, reduction of volume and weight, and reduction of potential fire and environmental hazards. Therefore, HTS transformers attract much attention all over the world. In 1996, a single-phase HTS transformer was successfully developed in collaboration by Kyushu University, Fujitsu Electric Co., Ltd and Sumitomo Electric Industries in Japan. The transformer operated at 77 K, with capacity 500 kVA, voltage 6.6 kV/3.3 kV and current 76 A/152 A. Moreover, a capacity of 800 kVA was achieved when operating in 66 K temperature [4]. ABB of Switzerland and AMSC of America first developed a three-phase distribution HTS transformer with capacity 630 kVA, voltage 18.72 kV/0.42 kV and current 11.2 A/866 A, which had successfully operated in a live grid of Geneva for one year in 1997 [6]. After finishing a single-phase HTS transformer with capacity 100 kVA and voltage 5.5 kV/1.1 kV, Siemens of Germany developed an HTS transformer (including cooling system) with capacity 1 MVA and voltage 25 kV/1.4 kV that was used in a locomotive system in 2001. The conventional electrical and thermal tests, such as no-load and load loss, were performed at 67 K, 50 Hz and 16.7 Hz respectively. Compared with a conventional locomotive transformer, HTS transformer weight and volume were reduced by 45% and 40% respectively. Efficiency improved from 92%–95% to 99%, while about 30% of

energy consumed in the whole driving system can be saved [11,12]. In May 1998, American Electric Company collaborated with IGC and Oak Ridge National Laboratory completed a single-phase HTS transformer with capacity 1 MVA and voltage 13.8 kV/6.9 kV [5]. Furthermore, Oxford Instrument Company (England) and Electrical Engineering Laboratory of Grenoble (France) together designed a single-phase HTS transformer with capacity 41 kVA and voltage 2.1 kV/0.4 kV that was supported by the European Ready Project. The cooling core structure was placed in its magnetic circuit, and its primary windings were wound by so-called first generation HTS Bi2223/Ag tapes manufactured by PIT, while secondary windings were wound using the second HTS YBCO tapes with 60 m in length [13].

In 2003, a three-phase HTS transformer with capacity 26 kVA, voltage 400 V/16 V, and current 37.53 A/938.2 A was first produced to study its magnetic-thermal stability when operated at a rated current [14,15]. A single-phase HTS transformer with capacity 45 kVA and voltage 2.4 kV/0.16 kV was developed in 2005 in an attempt to evaluate its mechanical stability during extreme operating conditions such as a lightning impulse and sudden short circuit [16]. The two model HTS transformers accumulate rich experience in the development of a 630 kVA/10.5 kV three-phase HTS transformer.

The design, fabrication and test of a 630 kVA 10.5 kV/0.4 kV three-phase HTS power transformer with amorphous alloy cores are presented in this article. The transformer is the second worldwide HTS transformer operated in a live grid after the one developed by ABB.

2 Design of HTS transformer

A superconducting transformer mainly consists of windings, an iron core, non-metal cryostat, current leads, cryo-cooled system, level meter and on-line measuring system. Based on geometrical, electro-magnetic and mechanical characteristics of HTS tapes, the structure of HTS transformer windings are solenoid and double-pancakes. Generally, the solenoid winding is suitable for high voltage (HV) windings with numerous turns and the double-pancake windings connected in parallel is adapted to low voltage (LV) windings with large current.

2.1 Design of iron core

The state-of-the-art amorphous alloy core, whose loss is less than 70% of the conventional iron core, was chosen as the iron core of the transformer. However, the amorphous alloy core is fragile and cannot endure external forces. Its performance can also be affected by self-weight, which is also one of the reasons why the amorphous alloy core has not yet been used in large-scale transformers. Additionally, its flux density is only 1.275 T, which is much lower than that of conventional iron core. Therefore, supporting and reinforcing measures on the amorphous alloy core must be taken carefully in its design, processing and installation. Convoluted amorphous alloy core of the 630 kVA HTS transformer has 5 limbs with 3 phases. The design parameters of the core are listed in Table 1.

Table 1 Specifications of amorphous core

parameter	value
types/materials	convoluted core of 5 limbs with 3 phases / amorphous alloy core
diameter/mm	396
net cross-section/cm^2	815.03
height (H_w)/mm	870
width (M_o)/mm	780
flux density/T	1.275
turn voltage/($V \cdot turn^{-1}$)	23.09
weight/kg	3736
no-load loss/W	1031.1

2.2 Design of HTS transformer windings

2.2.1 Properties of HTS tapes and insulation

The hermetic stainless steel-reinforced 55-filament Bi2223/Ag tape used in the three-phase 630 kVA HTS power transformer is produced by American Superconductor (AmSC). The minimum critical current of the tape is 115 A at 77 K and self-field, and its main performance is listed in Table 2. The authors developed a wrapping machine that can be used to wrap the tape automatically with single, double and triple wrapping by polyimide films. The machine for winding insulation and the wound insulation HTS tape are shown in Figs. 1(a) and 1(b), respectively. There is no degradation of critical current in the HTS tape at 77 K and self-field before and after the insulation, which shows that the insulation technology is safe and suitable.

Table 2 Specifications of Bi-2223 HTS tape

parameter	value
tape thickness/mm	0.32(+/–0.02)
tape width/mm	4.8(+/–0.2)
filament number	55
critical current*/A	> 115
maximum rated tensile stress**/MPa	265
maximum rated tensile strain**/%	0.4
minimum bend diameter**/mm	70
hermetic performance	withstand 16 hours on 30 standard atmosphere in liquid nitrogen (LN_2)

* 77 K, self-field, ** 95% critical current degradation

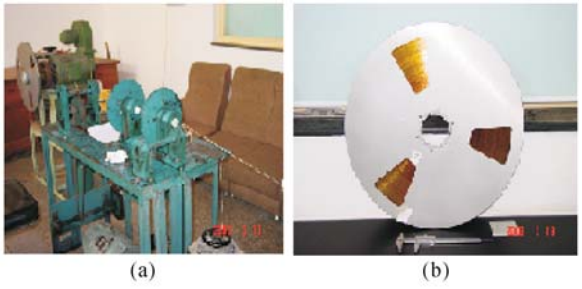

Fig. 1 Machine for winding insulation of HTS tape. (a) Winding apparatus; (b) wound insulation of HTS tape

After the winding and insulation of the HTS tapes, the withstand voltages among turns and between layers were tested at 77 K temperature. According to design experience for a conventional transformer, the voltage between layers is very high if HV windings are of the solenoid type. Thus, it is necessary to insert 5 layers with 40 μm thick polyimide films or 6 layers with 0.05 mm thick NOMEX papers as insulation between neighboring layers (no stay). The withstand voltages among turns and between layers at 77 K temperature are shown in Fig. 2. The withstand voltages among turns is more than 12 kV, which fully satisfies the needs of the withstand level in turns. The 'crossing' wrapping insulation technology was chosen to increase the reliability of insulation in turns, which is more reasonable in insulating techniques. Based on the provision of GB1094.3–85, lightning impulse withstand voltage in rated 10 kV HV windings should withstand 75 kV (peak value). The maximum lightning impulse voltage between layers is 9.375 kV, provided that inceptive wave distribution in solenoid windings is linear. 40 μm thick polyimide film per layer and 0.05 mm thick NOMEX T410 paper are chosen as layer insulation, respectively. The withstand voltage between layers at power frequency was then tested at 77 K temperature, of which the results are shown in Fig. 3. These results indicate that the withstand voltage between layers approaches saturation when the number of insulation layers is 6. Therefore, insulation thickness with 6 layers was chosen between layers. Based on the test results, the withstand voltage strength between layers is about 25 kV, which adequately satisfies the reliable requirement of layer insulation.

2.2.2 Design of HTS transformer windings

Since the windings and iron core of a superconducting transformer operate at different temperatures, i.e., the windings operate at liquid nitrogen temperature and iron core operates at room temperature, the structure of a superconducting transformer is similar to the conventional dry-type transformer. The HV windings of an HTS

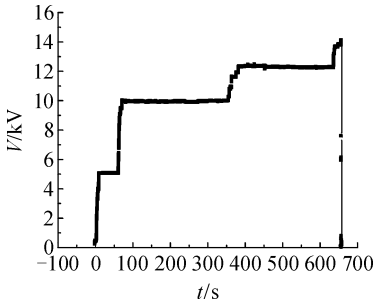

Fig. 2 Breakdown voltage between turns

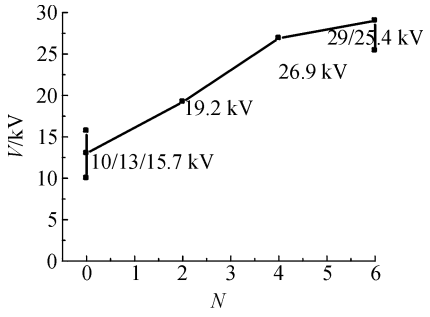

Fig. 3 Breakdown voltage between layers

transformer are solenoid, consisting of 8 layers that are divided into 4 groups. Each group is composed of 2 layers, between which there is insulation of 6 layer polyimide films. There is a cooling channel with cross-section of 10 mm × 0.2 mm between each group. The LV winding is double-pancake, consisting of 23 double-pancakes connected in parallel. Each double-pancake has 10 turns. The HTS tapes in windings are exposed to an external magnetic field that is mostly axially parallel (axial) to the tape wide plane, although there is a significant radial component (radial) perpendicular to the tape plane on both edge parts. Moreover, the radial component is much larger than the axial component on the edges. Since HTS tapes have strong anisotropic characteristics at 77 K, critical current significantly degrades with an increase of the magnetic field perpendicular component, which also results in alternating current (AC) loss to increase in the windings. All the windings are then wound with a strand composed of two parallel-transposed multi-filamentary tapes to ensure a uniform current distribution, prevent unbalanced current flow and reduce AC losses [17]. Solenoid and double pancake windings are cylindrically concentric. The LV winding is located coaxially outside its HV counterpart. The total length of the tape is 5.1 km. Because the configuration of the iron core is 3 phases with 5 limbs, a balanced winding is necessarily appended in the core. The balanced winding is wound by copper wire with a diameter of Φ8 –10 mm and a total length of 82 m. Main geometrical parameters of HTS windings are presented in Table 3.

Table 3 Main geometrical parameters of HTS windings

winding name	parameter	type and value
HV	winding type	solenoid
	layer No.	8
	turn No.	262
	diameter (inner/outer)/mm	488/504
	height/mm	342.5
LV	winding type	double-pancake
	double-pancake No.	23
	turn No.	10
	diameter (inner/outer)/mm	581/608
	height/mm	355
balanced winding	winding type	solenoid
	diameter (inner/outer)/mm	400/440
	layer No.	2
	turn No.	10
	height/mm	122.4

2.2.3 Fabrication of HTS windings

A primary winding consists of 8 layers, where every two layers contain a stay made of insulation cardboard, and spacer bars with a cross-section of 10 mm × 2 mm are uniformly arranged along the radial direction. An insulation paper with 6 layers is used between layers of HV winding. The bobbin of HV and LV windings are made of glass fiber reinforced plastics (GFRP) with 5 mm in thickness. On the outer surface of the bobbin, there are many axial grooves through which liquid nitrogen can flow smoothly. In the process of winding, transposition is completed. An ordinary winding machine is used. The prestress must be smaller than the maximum-rated tensile stress of HTS tapes during the winding; otherwise the properties of the HTS will be mechanically damaged irreversibly. Figure 4 is an overview of the completed single-phase HTS transformer winding.

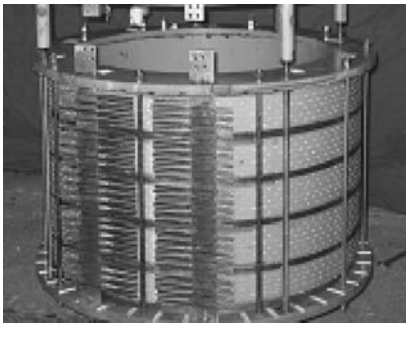

Fig. 4 Overview of single-phase transformer winding

2.3 Design of HTS transformer cryostat

Since HTS windings operate at low temperature, an HTS transformer can be easily produced if both iron core and windings are placed in a low temperature environment, i.e., the so-called cooled iron core structure, which is similar with that of the conventional dry transformer. Since there is always a no-load loss in the iron core of transformers and the resistivity of iron core is significantly decreased at low temperature, there is a major increase of eddy-current loss in the iron core. Since 1 W power consumed at 77 K temperature is equivalent to 15 W power consumed at room temperature, a huge loss will bring an immense load to the cryo-cooling system and significantly reduce the efficiency of the HTS transformer. Therefore, windings and iron core must be separated, i.e., HTS windings are located in a cryostat system separated from the iron core operating at room temperature.

There are three kinds of heat exchange: solid conduction, convection and thermal radiation. The amount of heat exchange is proportional to the conduction cross-section. Reducing the cross-section can reduce heat by solid conduction. Convection comes from the collision of gas molecules, by which heat automatically transfers from a high temperature zone to one at low temperature. High vacuum can reduce heat transfer by convection. As long as the temperature is above 0 K, any material can radiate heat outwards. Glazed metal foil can reflect the radiation effectively and reduce heat-leakage by thermal radiation. Conventional cryostat is made of high-strength stainless steel, and the wall of the cryostat may be very thin and can thus effectively reduce heat-leakage by solid conduction. On the other hand, stainless steel is high in tightness and does not deflate. The cryostat made of stainless steel can therefore maintain a vacuum, which greatly reduces heat-leakage from the convection. There are multi-layers of wrapping glazed metal foil between the inner and outer walls of the cryostat, and they are useful for preventing heat radiation from the environment. At the same time, a certain amount of active carbon is inserted into the space between the inner and outer walls to absorb remanent gas molecules. Therefore, the conventional cryostat is generally made of stainless steel material and thus has advantages of high strength, the ability to maintain a vacuum over a long period of time, and good thermal insulation. The vacuum of this cryostat can be pumped down to 10^{-7} Pa and can maintain this level for more than 2 years. However, because the cryostat of a superconducting transformer surrounds the magnetic circuit, this kind of cryostat cannot be made of metal materials wherein a large amount of eddy current will be induced. GFRP, with excellent insulation, is a kind of available candidate material used to make the cryostat of superconducting transformers. Different from the conventional cryostat, the radiation-protection shield between the inner and outer walls is made of glazed thin metal foil with cuts to prevent

the foil from forming a short circuit current. The schematic structure is shown in Fig. 5. Figure 6 is a photo of the real cryostat made of GFRP. Unfortunately, since GFRP has intrinsic characteristics of air-bleed, the vacuum of the cryostat cannot last a long time, and thus needs pumping periodically. Active-carbon is usually used as gas absorption material between the inner and outer walls of the conventional cryostat. Semiconductors cannot be used as gas absorption material to avoid short circuit between the walls of the cryostat. Therefore, in the cryostat of superconducting transformers, organic materials should be chosen as gas absorption material that can avoid all of the above disadvantages. Additionally, since the cryostat of a superconducting transformer operates in an AC magnetic field environment, any magnetic material should not be used in the design and fabrication of the cryostat.

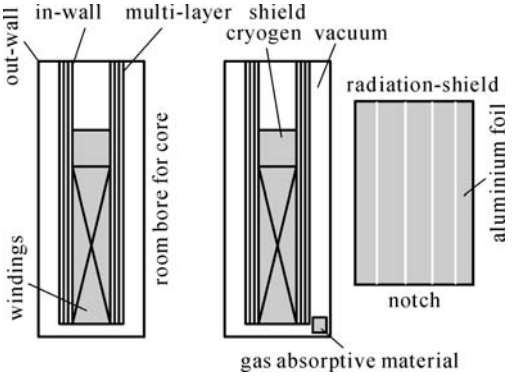

Fig. 5 Schematic view of GFRP Dewar

Fig. 6 Photograph of GFRP Dewar

2.4 Design of current leads

Since the cross-sections of secondary current leads are about 26 times larger than those of primary ones, heat-conduction in primary leads is very small compared with their secondary counterparts. The design of current leads focuses on current leads of LV windings. Because of the large current in LV windings, the current lead that introduces and transits electric current from room temperature to cryogenic temperature is generally made of copper. A loss that includes heat-leakage and joule loss in current leads is the main component of all losses in HTS transformers. A current lead with a large cross-section will result in the reduction of joule loss, but conduction heat-leakage will increase because conduction heat-leakage is proportional to the cross-section. In contrast, a current lead with a small cross-section can reduce conduction heat-leakage while joule loss will increase. A compromising and optimum design of current lead is very important for HTS transformers.

The cross-section of an LV current lead should be optimized to reduce joule loss and heat-leakage into the cryostat, to minimize heat-leakage from the room temperature part to the low temperature part.

Therefore, the current leads of secondary windings are chosen as traditional gas-cooled current leads to reduce heat-leakage into liquid nitrogen. The optimum design of current lead is found based on one-dimensional equation:

$$\frac{\mathrm{d}}{\mathrm{d}z}\left[Ak(T)\frac{\mathrm{d}T}{\mathrm{d}z}\right] - \dot{m}_I\, c_p(T)\frac{\mathrm{d}T}{\mathrm{d}z} + \frac{\rho(T)I_t^2}{A} = 0, \quad (1)$$

where A is cross-section, $k(T)$ denotes thermal conductivity, $c_p(T)$ is specific heat, $\rho(T)$ is resistivity, T is the temperature along the lead, I_t is transport current, and $\dot{m}_I$ is the mass flow rate of the boiled cryogen gas. The optimized cross-section of the current lead is about 60 mm^2 by means of simulation. Figure 7 illustrates the test results of heat-leakage with different input losses, which simulates load loss of the transformer, while the abscissa and vertical-coordinate represent simulated load loss and evaporation of liquid nitrogen per hour respectively. The results indicate that the optimum cross-section of the current lead is 64 mm^2 close to the simulation. As a result, the cross-section of the LV windings is chosen to be 65 mm^2 in the proposed HTS transformer.

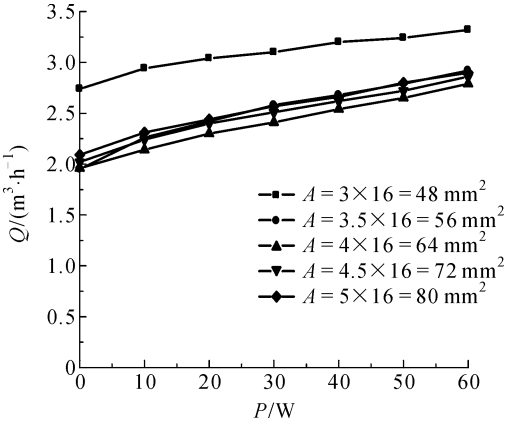

Fig. 7 Optimized cross-section of current lead

2.5 AC loss analysis of HTS windings

Although there is no loss in the superconducting state and direct current (DC) operating mode in superconductors, an AC loss appears if it carries AC current or locates in an AC magnetic field environment, since the flux-pinning effect exerts viscous force on the flux line. AC losses in composite superconductors consist of three kinds of losses: hysteretic loss, eddy current loss and coupling loss. Among them, the first is the dominant and is proportional to the frequency, while the latter two are proportional to the square of the frequency. AC losses are the main heat source of windings during their operation and have significant effect on winding stability, Thus, it is indispensable to analyze their effects in detail to assure the stable and safe operation of HTS windings. Because HTS tapes of windings are exposed to AC magnetic fields that consist of parallel and perpendicular components, and windings carry AC current that has the same phase with the magnetic field, plus their strong anisotropic characteristics at 77 K temperature, AC loss calculation of HTS tapes is much more complicated than joule loss calculation of conventional conductors.

1) Hysteretic loss

While HTS tape is exposed to perpendicular AC magnetic field, hysteretic loss is given by [17,18]

$$P_{\perp} = Kf\frac{w^2\pi}{\mu_0}B_c^2\beta_{\perp}\left(\frac{2}{\beta_{\perp}}\ln(\cosh\beta_{\perp}) - \tanh\beta_{\perp}\right), \quad (2)$$

where K is geometrical factor; w is tape width; B_c is characteristic parameter, $B_c = \mu_0 J_c d/\pi$; $\beta_{\perp}$ is normalized perpendicular magnetic field, $\beta_{\perp} = B_{\perp}/B_c$; and $B_{\perp}$ is the amplitude of perpendicular magnetic field. Referring to stainless steel-reinforced multi-filamentary Bi2223/Ag tapes manufactured by AmSC, K is chosen to be 1.35.

If the HTS tape carries AC current and is simultaneously exposed to the AC parallel magnetic field that has the same phase with the AC current, AC loss per unit length is [19,20]

$$P_{//} = \begin{cases} \dfrac{2fCAB_p^2}{3\mu_0}(i^3 + 3\beta_{//}^2 i), & \beta_{//} < i, \\ \dfrac{2fCAB_p^2}{3\mu_0}(\beta_{//}^3 + 3\beta_{//} i^2), & i < \beta_{//} < 1, \\ \dfrac{2fCAB_p^2}{3\mu_0}\left[\beta_{//}(3+i^2) - 2(1-i^3) + 6i^2\dfrac{(1-i)^2}{(\beta_{//}-i)} - 4i^2\dfrac{(1-i)^3}{(\beta_{//}-i)^2}\right], & \beta_{//} > 1, \\ \dfrac{2fCAB_p^2}{3\mu_0}[\beta_{//}(3+i^2) - 2(1-i^3)], & \beta_{//} >> 1, \end{cases} \quad (3)$$

where f, B_p, CA are frequency, completely penetrated field and superconducting effective cross-section, respectively; $\beta_{//}$ is the normalized parallel magnetic field, $\beta_{//} = B_{//}/B_p$; i is normalized amplitude of transport current $i = I_p/I_c$; I_c is critical current; and I_p is the amplitude of transport current.

2) Coupling loss

The coupling current is induced because of the couple among HTS filaments through the metal matrix in composite HTS tapes under AC magnetic field condition. The filaments are surrounded by metal matrix; the coupling current transversally flows through the metal matrix and then induces a coupling loss:

$$P_c = \eta_c\frac{AB_a^2}{2\mu_0}\left[\frac{n_s\omega^2\tau}{1+(\omega\tau)^2}\right], \quad (4)$$

where η_c, defined as the ratio of HTS filament volume to total composite volume, is the volume factor of composite HTS tape; n_s is the shape factor of filament, A is cross-section and τ is coupling characteristic time constant respectively.

3) Eddy current loss

Practical HTS tapes are composite fabricated by powder-in-tube (PIT), in which superconducting filaments are inserted into the metal matrix. The eddy current can then be induced in the metal so that eddy current loss is produced if the composite is exposed to an AC magnetic field:

$$P_e = \frac{2B_a^2}{\mu_0}\left[\frac{\mu_0\omega^2 w^3 d}{48\rho_s}\right]. \quad (5)$$

The term in square brackets is the loss function independent of amplitude of magnetic field and is proportional to the square of frequency. Here, w represents tape width and d refers to its thickness in the case of a perpendicular field; otherwise, w represents thickness and d refers to width in the case of parallel field; ρ_s is effective resistivity of the metal matrix. The eddy current loss in an AC perpendicular field is much higher than that in an AC parallel field at power frequency, and the loss is comparable with that in very high parallel fields. However, the mutual-shielding effect between superconductor and

metal matrix reduces the hysteretic and eddy current loss. It is obvious that the eddy current loss is inversely proportional to the effective resistivity ρ_s. Increasing the resistivity of the metal matrix is an effective means of reducing eddy current loss. At present, silver-magnesium alloy and stainless steel are used as sheath/matrix of composite HTS tapes, which simultaneously increases mechanical strength and resistivity of the matrix and thus significantly reduces the eddy current loss. Therefore, the total AC loss of the HTS windings is the sum of the above loss components:

$$P_T = P_{\perp} + P_{//} + P_c + P_e. \quad (6)$$

2.6 Installation and test of HTS transformer

Based on earlier analysis and the magnetic field distribution simulated by finite element method (FEM), the main design parameters of the 630 kVA HTS transformer are summarized in Table 4.

Table 4 Main design parameters of HTS transformer

parameter		design value
winding voltage (HV/LV)/kV		10.5/0.4
winding current (HV/LV)/A		34.64/909.33
balanced winding voltage /V		230
balanced winding current/A		228
iron core	diameter/mm	396
	height (H_W)/mm	870
	width (M_o)/mm	780
	flux density/T	1.275
cryo-stat	diameter (inner/outer)/mm	410/760
	height/mm	680
operating temperature/K		77
operating frequency/Hz		50
% impedance		2.45%
vector group		Yyn0 + d7
max leak flux/mT		65.6

After finishing the design and manufacture of components, the HTS transformer was installed. The level of the liquid nitrogen in the cryostat is measured by a level meter to assure that HTS windings operate in a superconducting state at 77 K all the time. Figure 8 is an overview of the developed 630 kVA three-phase HTS transformer with amorphous alloy core installed in the GFRP cryostat. To our knowledge, the amorphous alloy core is the largest in the world.

The basic routine tests of the HTS transformer were performed in the Xinjiang Transformer Factory, TBEA, Changji, Xinjiang. All of the tests were managed by experts from the China National Transformer Quality Supervision Testing Center, Shenyang. The routine tests include DC resistances of windings, transformation ratio, symbol identification of vector group, insulation resistance of windings, insulation resistance of iron core, no-load current, no-load loss, external withstand voltage, inductive withstand voltage, short circuit impedance and load loss. Real tests include a temperature rise in the amorphous core. Special tests include null impedance in the three-phase transformer, and a load test with loading up to 1.1 times the rated level for an extended period. The DC resistances of windings are summarized in Table 5, while other results are listed in Table 6. After considering heat-leakage of the cryostat, current lead and various losses which are converted to loss value at room temperature, the efficiency of the HTS transformer is 98.5%, higher than the 98.1% in the conventional dry transformer with the same scale. Since HTS windings operate in liquid nitrogen temperature of 77 K all the time, the temperature rise tests mainly include temperature rise of the iron core and lead terminals. In the no-load test, the temperature of the LV lead terminal is almost constant, but that of the HV lead terminal approached room temperature and was not affected by the temperature of the iron core. However, the temperature of the iron core increased with time at first and stably reached 50°C. In the load test, load loss was constant; a stable temperature rise of 32°C of iron core was achieved after operating for 16 hours; the temperature of the HV current terminal was 21°C, slightly higher than the 18°C of the environment. However, temperature rise of the LV lead terminal rapidly increased in the first two hours, then increased slowly and finally reached equilibrium with temperature of 27.5°C. For the lightning impulse test, an HV winding mode exactly the same as that of the 630 kVA HTS transformer was fabricated and tested by Shenyang Transformer Group, Tebian Electric Apparatus Stock Co., Ltd (TBEA). The results show that the lightning impulse withstand voltage reached 155 kV more than the Chinese National Standards of 75 kV with the related scale. For the sudden short circuit test, a 45 kVA single-phase HTS transformer based on the same technology of 630 kVA HTS windings was developed and tested at the China National Transformer Quality Supervision Testing Center, Shenyang [16]. All of the results lay the foundation and accumulate

Fig. 8 Overview of HTS transformer

valuable knowledge on the target 630 kVA HTS transformer, which also ensure the safety and reliability of the transformer operation. Consequently, the developed 630 kVA HTS transformer meets the requirements of test operations in a live grid.

Table 5 DC resistances of HTS windings

temperature	HV winding/Ω	LV winding/Ω
room temperature	12.49	1.25×10^{-2}
77 K	$2.65 \times 10^{-3*}$	$1.32 \times 10^{-4*}$

* Resistances of the HTS windings should be zero at 77 K; these values in Table originate from copper lead and joint resistance

Table 6 Main parameters of HTS transformer

parameter	design value	test value
capacity/kVA	630	630
no-load test		
excited current	1.15%	1.36%
transformation ratio	26.25	26.25
core loss*/W	1031.1	1090
load test		
% impedance	2.45%	2.74%
winding loss**/W	121.8	110.67
inductive withstand voltage	100 Hz, 30 s	pass
insulation level	HV 28 kV 60 s LV 5 kV 60 s balanced 5 kV 60 s	pass
rush current	10 times rush current 0.2 s	no-quench

* room temperature, ** 77 K temperature

3 Operation in live power grid

The HTS transformer operated in a power grid after various testing and authorization in the city of Changji, Xinjiang, northwest of China, serving a TBEA cable manufacturing plant. The operation scene is shown in Fig. 9. The operation system consists of the HTS transformer, main control room (detecting and measuring the level of liquid nitrogen in the winding of the cryostat) and liquid nitrogen tank. The open cooling cycle is supplied by an external liquid nitrogen container for compensating the evaporated nitrogen.

Several protective measures, such as short-circuit breakers with a break delay of 100 ms, nitrogen level, etc. were taken to ensure the transformer's reliable operation. The open cooling cycle is supplied by a volume 6 m^3 external liquid nitrogen tank for compensating the evaporated nitrogen due to winding loss, heat-leakage of current leads and natural evaporation of cryostat. During the first 0.2 s when the transformer is switched on, there is an in-rush of current, of which the peak can reach values 10 times above the rated current, and there is no quench in HTS windings. This indicates that the transformer could operate safely in the power live grid.

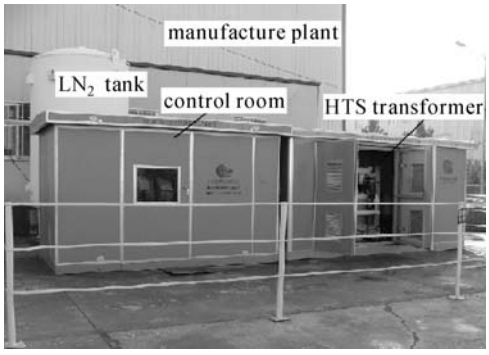

Fig. 9 HTS transformer operation field serving TBEA cable manufacture plant (Changji, Xinjiang)

On November 11, 2005, the 630 kVA HTS transformer was operated in a live power grid of Changji, Xinjiang, northwest of China, serving a TBEA cable manufacture plant. In the period of operation, there was no fault, showing that the transformer could operate with high reliability.

4 Conclusions

A three-phase 630 kVA HTS transformer with an amorphous core at room temperature was developed and tested for operating characteristics. It was successfully operated in a power live grid and had long-term operational reliability.

The transformer losses including core loss, AC losses in the superconducting windings and current leads are systematically analyzed in detail. The AC losses in windings are of the same magnitude of order with the current leads. The efficiency of the transformer is estimated to be 98.5%, considering those losses and the coefficient of penalty in a rated operation.

The cooling mode was operated with an open cooling cycle in the HTS transformer, in which liquid nitrogen was at the boiling point temperature of 77 K. To prevent the electric field from focusing on the boiling nitrogen gas bubble, future commercial HTS transformers should operate in sub-cooled liquid nitrogen under 77 K with closed cryo-cooler recycling.

The high price of HTS tape is always the leading obstacle of HTS commercialization. The cost of Bi2223/Ag tapes amounts to 70%–80% of the whole price of HTS transformers. Based on evaluation, the HTS transformer has economical advantages over the conventional transformer when its capacity is more than 5 MVA.

The shape of a commercial HTS tape has a large aspect

ratio over 10. There is no problem for low or middle voltage level applications below 35 kV, but it presents serious challenges for high voltage level applications above 110 kV. Examples are the point-discharging phenomena and insulation material aging, which subsequently shorten the lifetime of insulation materials and even destroys winding insulation. On the other hand, the insulation technology at low temperature also needs to be emphasized in superconducting power applications in the near future because the performance of the conventional insulation materials at low temperature is better than that at room temperature.

Leak field is a serious issue in HTS transformers with large capacity, in which the radial leak field is more than 200 mT and the axial leak field is even up to 500 mT, which will result in serious critical current degradation of HTS tapes. If cooled by sub-cooled liquid nitrogen such as 65 K, the critical current of HTS tape will be double critical current at 77 K. The amount of HTS wire will be reduced and the capacity of the transformer will correspondingly increase (ability to overload), the AC losses of windings will be also great reduced.

Reinforcing components consisting of GFRP in HTS windings should be used instead of conventional metal components to avoid creating suspension potential and partial discharge. Heat-leakage of cryostat is one of the loads of the cooling system, which directly has influence on the operational efficiency of the superconducting transformer. For large capacity superconducting transformers, the cryostat should have a structure in which all the windings are in one cryostat with three room temperature bores for the iron core, so that the number of current lead terminals from the cryostat can be reduced and consequently the load of the cryo-cooler can also be reduced. In addition, it is convenient for setting up regulating winding and designing a tap switch to meet the needs of regulating voltage in power systems. Choosing this structure of the cryostat can increase its degree of vacuum level and then reduce heat-leakage.

Since HTS tape is strongly anisotropic, the critical current significantly degrades in the perpendicular field, which consequently reduces current carrying capability and increases winding AC losses. The radial leakage magnetic field components should be as small as possible in the design of HTS transformers. The magnetic-shielding screens with cut are installed at the two ends of the windings, which can alter the path of leakage magnetic field and then effectively reduce radial magnetic field components.

In the design of high voltage or super high voltage conventional transformers, structures of HV windings are generally interleaved-continuous, interleaved or inserted shielding to improve on-wave-process distribution. For HTS transformers, interleaved techniques are not available because of intrinsic characteristic limits of HTS tapes themselves. Therefore, the inserted shielding windings should be used so that capacitance in windings is compensated, and thus improve on-wave distribution and enhance the strength of the lighting impulse withstand.

Acknowledgements This work was supported by the Ministry of Science and Technology of China (2002AA306381), Tebian Electric Apparatus Stock Co., Ltd (TBEA) and the '100 Talents Project' of Chinese Academy of Sciences, China (0640111C11).

References

1. Tsukamoto O. Roads for HTS power applications to go into the real world: Cost issues and technical issues. Cryogenics, 2005, 45(1): 3–10
2. Furuse M, Fuchino S, Higuchi N. Investigation of structure of superconducting power transmission cables with LN_2 counter-flow cooling. Physica C, 2003, 386: 474–479
3. Lin Y B, Lin L Z, Gao Z Y, Wen H M, Xu L, Shu L, Li J, Xiao L Y, Zhou L,Yuan G S. Development of HTS transmission power cable. IEEE Transactions on Applied Superconductivity, 2001, 11(1): 2371–2374
4. Funaki K, Iwakuma M, Kajikawa K, Takeo M, Suehiro J, Hara M, Yamafuji K, Konno M, Kasagawa Y, Okubo K, Yasukawa Y, Nose S, Ueyama M, Hayashi K, Sato K. Development of a 500 kVA-calss oxide-superconducting power transformer operated at liquid-nitrogen temperature. Cryogenics, 1998, 38(2): 211–220
5. Schwenterly S W, McConnell B W, Demko J A, Fadnek A, Hsu J, List F A, Walker M S, Hazelton D W, Murray F S, Rice J A, Trautwein C M, Shi X, Farrell R A, Bascuhan J, Hintz R E, Mehta S P, Aversa N, Ebert J A, Bednar B A, Neder D J, McIlheran A A, Michel P C, Nemce J J, Pleva E F, Swenton A C, Swets W, Longsworth R C, Johsnon R C, Jones R H, Nelson J K, Degeneff R C, Salon S J. Performance of a 1-MVA HTS demonstration transformer. IEEE Transactions on Applied Superconductivity, 1999, 9(2): 680–684
6. Zueger H. 630 kVA high temperature superconducting transformer. Cryogenics, 1998, 38(11): 1169–1172
7. Hatta H, Nitta T, Oide T, Chiba M, Shirai Y, Mochida A. Experimental study on characteristics of superconducting fault current limiters connected in series. Superconductor Science & Technology, 2004, 17(5): 276–280
8. Elschner S, Breuer F, Noe M, Rettelbach T, Walter H, Bock J. Manufacturing and testing of MCP 2212 bifilar coils for a 10 MVA fault current limiter. IEEE Transactions on Applied Superconductivity, 2003, 13(2): 1980–1983
9. Barnes P N, Sumption M D, Rhoads G L. Review of high power density superconducting generators: Present state and prospects for incorporating YBCO windings. Cryogenics, 2005, 45(10-11): 670–686
10. Luongo C A, Baldwin T, Ribeiro P, Weber C M. A 100 MJ SMES demonstration at FSU-CAPS. IEEE Transactions on Applied Superconductivity, 2003, 13(2): 1800–1805
11. Meinert M, Leghissa M, Schlosser R, Schmidt H. System test of a 1-MVA-HTS-transformer connected to a converter-fed drive for rail vehicles. IEEE Transactions on Applied Superconductivity, 2003, 13(2): 2348–2351

12. Schlosser R, Schmidt H, Leghissa M, Meinert M. Development of high-temperature superconducting transformers for railway applications. IEEE Transactions on Applied Superconductivity, 2003, 13 (2): 2325–2330
13. Tixador P, Donnier-Valentin G, Maher E. Design and construction of a 41 kVA Bi/Y transformer. IEEE Transactions on Applied Superconductivity, 2003, 13(2): 2331–2336
14. Wang Y S, Zhao X, Li H D, Lu G H, Xiao L Y, Lin L Z, Guan Y, Bao Q, Xu X, Zhu Z Q, Wang Z K, Dai S T, Hui D. Development of solenoid and double pancake windings for a three-phase 26 kVA HTS transformer. IEEE Transactions on Applied Superconductivity, 2004, 14(2): 924–927
15. Wang Y S, Zhao X, Li H D, Lu G H, Xiao L Y, Lin L Z, Hui D, Dai S D, et al. A three-phase 26 kVA HTS power transformer. In: Proceedings of the Twentieth International Cryogenic Engineering Conference (ICEC20). Elsevier, 2005, 693–696
16. Wang Y S, Han J J, Zhao X, Li H, Guan Y, Bao Q, Xiao L, Lin L, Zhu Z, Dai S, Hui D. Development of a 45 kVA single-phase model HTS transformer. IEEE Transactions on Applied Superconductivity, 2006, 16(2): 1477–1480
17. Iwakuma M, Nishimura K, Kajikawa K, Funaki K, Hayashi H, Tsutsumi K, Tomioka A, Konno M, Nose S. Current distribution in superconducting parallel conductors wound into pancake coils. IEEE Transactions on Applied Superconductivity, 2000, 10(1): 861–864
18. Magnusson N, Wolfbrandt A. AC losses in high-temperature superconducting tapes exposed to longitudinal magnetic fields. Cryogenics, 2001, 41(10): 721–724
19. Magnusson N. Semi-empirical model of the losses in HTS tapes carrying AC currents in AC magnetic fields applied parallel to the tape face. Physica C, 2001, 349(3-4): 225–234
20. Rabbers J J, van der Laan D C, ten Haken B, ten Kate H H J. Magnetisation and transport current loss of a BSCCO/Ag tape in an external AC magnetic field carrying an AC transport current. IEEE Transasctions on Applied Superconductivity, 1999, 9(2): 1185–1188